



## RESEARCH LETTER

10.1002/2017GL075618

## Key Points:

- We explore the relationship between ozone, summer ASL, and fall sea ice
- Our model shows ozone-induced ASL trends and captures observed ASL/sea ice relationships
- Our model, however, does not reproduce the observed austral fall regional sea ice trends

## Supporting Information:

- Supporting Information S1

## Correspondence to:

L. Landrum,  
landrum@ucar.edu

## Citation:

Landrum, L. L., Holland, M. M., Raphael, M. N., & Polvani, L. M. (2017).

Stratospheric ozone depletion: An unlikely driver of the regional trends in Antarctic sea ice in austral fall in the late twentieth century. *Geophysical Research Letters*, 44, 11,062–11,070. <https://doi.org/10.1002/2017GL075618>

Received 11 SEP 2017

Accepted 6 OCT 2017

Accepted article online 11 OCT 2017

Published online 11 NOV 2017

## Stratospheric Ozone Depletion: An Unlikely Driver of the Regional Trends in Antarctic Sea Ice in Austral Fall in the Late Twentieth Century

Laura L. Landrum<sup>1</sup> , Marika M. Holland<sup>1</sup> , Marilyn N. Raphael<sup>2</sup>, and Lorenzo M. Polvani<sup>1,3,4</sup> 

<sup>1</sup>National Center for Atmospheric Research, Boulder, CO, USA, <sup>2</sup>University of California, Los Angeles, CA, USA, <sup>3</sup>Columbia University, New York, NY, USA, <sup>4</sup>Lamont Doherty Earth Observatory, Palisades, NY, USA

**Abstract** It has been suggested that recent regional trends in Antarctic sea ice might have been caused by the formation of the ozone hole in the late twentieth century. Here we explore this by examining two ensembles of a climate model over the ozone hole formation period (1955–2005). One ensemble includes all known historical forcings; the other is identical except for ozone levels, which are fixed at 1955 levels. We demonstrate that the model is able to capture, on interannual and decadal timescales, the observed statistical relationship between summer Amundsen Sea Low strength (when ozone loss causes a robust deepening) and fall sea ice concentrations (when observed trends are largest). In spite of this, the modeled regional trends caused by ozone depletion are found to be almost exactly opposite to the observed ones. We deduce that the regional character of observed sea ice trends is likely not caused by ozone depletion.

### 1. Introduction

Stratospheric ozone loss is considered to be the primary driver of late twentieth century climate change in the Southern Hemisphere (Polvani et al., 2011; Previdi & Polvani, 2014). The largest impacts of stratospheric ozone loss on the tropospheric circulation occur during austral summer (December–January–February (DJF); Thompson et al., 2011), when positive DJF trends in the Southern Annular Mode (SAM), the leading climate mode of variability in the Southern Hemisphere, have been observed (see, e.g., Fogt et al., 2009). The SAM is known to affect the Amundsen Sea Low (ASL; Turner et al., 2013)—a zonally asymmetric region of low sea level pressure located in the high latitude South Pacific (~170–290°E and 60–75°S). Concurrent with twentieth century increases in DJF SAM, one would thus expect a deepening of the ASL, yet the depth and location of the ASL are highly variable, and observed twentieth century trends in ASL metrics are not robust over the satellite era (Turner et al., 2013). However, statistically significant trends in DJF ASL pressure emerge in climate model simulations when the entire time period of stratospheric ozone loss is considered—suggesting that the ASL may indeed have deepened in DJF in response to stratospheric ozone loss over the latter half of the twentieth century, albeit with a small magnitude relative to internal variability (England et al., 2016).

Changes in winds associated with the SAM are also believed to impact sea ice conditions. Previous work (e.g., Bitz & Polvani, 2012; Sigmond & Fyfe, 2010, 2014; Smith et al., 2012) has robustly shown that ozone loss, and the consequent increases in the SAM, drive an overall Antarctic sea ice *decline* in climate models. This decline results from increased upwelling of warm subsurface waters, which overwhelms the short-lived Ekman-induced cooling (Ferreira et al., 2015). This modeled response to ozone loss is difficult to reconcile with the observed increases in total Southern Hemisphere sea ice extent.

It is important to recall, however, that the total observed sea ice trends hide strong regional cancellations. Specifically, large increases in the Ross and Weddell seas are offset by large declines in the Amundsen–Bellingshausen Sea, with both of these trends being maximum in austral fall. Noting that this dipole pattern straddles the ASL, that the ASL is impacted by the SAM, and that the SAM is forced by ozone depletion, Turner et al. (2009), on the basis of evidence with an atmosphere-only model, suggested that the observed sea ice trends can be attributed to ozone depletion. Lefebvre et al. (2004) and Holland et al. (2016) also highlight that the nonannular component of the SAM (which is essentially a measure of the ASL) has a large influence on regional sea ice variations.

In this paper, focusing exclusively on the austral fall season (March–April–May (MAM))—when the largest observed sea ice trends are found—we ask the following questions: (1) can the regionality in twentieth century MAM sea ice trends be attributed to stratospheric ozone loss, and (2) if so, does ozone loss impact sea ice via the ASL? We answer these questions by analyzing two ensembles of model simulations with and without transient ozone changes. This allows us to clearly establish which regional sea ice trends, in our model, are caused by stratospheric ozone loss over the last half of the twentieth century. We then investigate the ASL role in producing these regional sea ice trends, through analysis of ASL–sea ice relationships, both in observations and in our model.

## 2. Data and Methods

As mentioned above, we focus here on MAM as this is the season of largest observed regional sea ice concentration (SIC) trends (e.g., Hobbs et al., 2016). Following England et al. (2016), we analyze two distinct time periods: the end of the twentieth century when observations and simulations overlap (1979–2005) and a longer period (1955–2005) meant to capture the entire anthropogenic formation of the ozone hole so as to maximize the amplitude of the ozone forcings.

For the observational component of this study, to document the historical variations, we use the monthly 1979–2005 sea level pressure and 10 m winds from the Interim European Centre for Medium-Range Forecasting (ECMWF, 2012) reanalysis (ERA-I; Dee et al., 2011) and sea ice concentrations from the SSMR/SSM/I Bootstrap satellite-derived sea ice concentration (Comiso, 2000, updated 2015).

For the modeling component of this study, we use the Community Earth System Model (CESM, version CESM1-CAM5; Hurrell et al., 2013). This model is a comprehensive atmosphere, land, ocean, sea ice model. The version used here is identical to the one employed by the CESM Large Ensemble Project and is fully documented in Kay et al. (2015). This is a CMIP5-class climate model, with a nominal 1° resolution in all components and 60/30 vertical ocean/atmosphere levels.

It is important to stress that that the CESM reproduces many of the observed statistics of the ASL (location and size as well as seasonal changes in magnitude and location) quite well, compared to many other climate models (England et al., 2016; Hosking et al., 2013). Relationships between summertime (DJF) ASL central pressure (when the ozone forcing of the SAM is the greatest and statistically significant) and sea ice concentrations in the CESM are evaluated in the CESM-LE preindustrial control run (PI). The PI consists of 1,800 simulation years at constant 1,850 (pre-industrial) external forcing. The PI interannual analyses serve as a basis for comparison with observed relationships between the ASL and sea ice. We also calculate correlations and regressions for CESM-PI time series of nonoverlapping decadal means of the 1800 year run and also running 40 year trends. Decadal regression coefficients from the CESM-PI analysis are in turn used with the CESM twentieth century simulations to attribute decadal changes in SICs to decadal changes in the ASL. All correlations and regressions are calculated on detrended time series.

To establish the impact of stratospheric ozone depletion, we compare two 8-member ensembles of twentieth century CESM simulations over the period 1955–2005. One ensemble has all the known historical forcings over the twentieth century (the “CESM-LE” ensemble; Kay et al., 2015). The other is identical in every respect, except that atmospheric ozone is held constant at 1955 levels (the “fixO<sub>3</sub>” ensemble). Each of the eight fixO<sub>3</sub> simulations is initialized from the corresponding member of the CESM-LE. See Figure 2a of England et al. (2016) for the ozone evolution in each ensemble. The impact of late twentieth century ozone is obtained by subtracting the means of the two ensembles.

To describe the ASL and its trends, we focus on the absolute central pressure as our key metric. This is defined as the minimum sea level pressure (SLP) in the Amundsen–Bellingshausen sea region between 170–290°E and 60–75°S. Both the magnitude and the location of the ASL-induced winds play roles in sea ice variability and trends (Hosking et al., 2013). The reason for focusing on the SLP metric alone is the following. After analyzing several ASL metrics, including its location, the absolute central pressure, and the relative central pressure (the minimum pressure after removing a regional mean, see Hosking et al., 2013), we found that it is the DJF absolute central pressure that has the strongest and most robust correlations with MAM sea ice in both the observations and the model.

### 3. Results

#### 3.1. Contrasting Observed and Simulated Twentieth Century Sea Ice Changes in MAM

Figure 1 presents late twentieth century SIC trends in MAM for the observations and our model ensembles. Like most CMIP5 models (e.g., Turner et al., 2015), the CESM-LE simulates a large sea ice loss throughout the Southern Hemisphere (SH), with particularly large decreases in SIC in the Ross and Weddell seas (Figures 1c and 1d). Simulated trends over the satellite era (1979–2005) are of the same sign but generally larger in magnitude than trends over the longer period 1955–2005. The key point, however, is that these negative modeled trends stand in stark contrast to the large positive trends in the observations in these regions (Figure 1a).

We now turn to the role of ozone depletion. Earlier studies have reported that ozone loss causes a decline in total SH sea ice extent (Bitz & Polvani, 2012; Sigmond & Fyfe, 2010, 2014; Smith et al., 2012). Our model results support this (Figures 1e and 1f). The novelty here is that we are now showing that the response to ozone loss has a distinctly regional pattern with the largest negative trends in the western Ross and the Weddell Seas. Smaller yet modestly positive trends are found in the Amundsen–Bellingshausen seas. This regional pattern of trends caused by ozone depletion is almost exactly *opposite* to the observed pattern over the satellite record (Figure 1a). Of particular note are the trends in the western Ross and the Weddell seas, which are large and positive in the observations: the trends caused by ozone depletion in our model simulation in those regions are strongly negative. And even in the Amundsen–Bellingshausen sector, the one location around Antarctica where the largest sea ice losses are observed, our model suggests that ozone may have caused some sea ice increase over the period 1955–2005 (Figure 1f). Hence, the suggestion of Turner et al. (2009) that ozone depletion may be responsible for some of the observed regional trends around Antarctica appears to be contradicted by our model results.

We summarize the findings for each sector by plotting the area-averaged SIC percentage changes in Figure 1b, for the period 1979–2005 (corresponding to the satellite era). The boxplot highlights the simulated pattern of mean sea ice loss in all regions for both the LE and LE-fixO3 ensembles. Internal variability in sea ice changes is substantial, particularly in the western Ross Sea, where some members in both the LE and LE-fixO3 ensembles have gains in sea ice although none reproduces the magnitude of the observed gains. The large internal variability also highlights the necessity of using an ensemble of simulations when teasing out the role of ozone in this complex system. The ensemble mean sea ice changes over the ozone depletion period (1955–2005) show decreases in the western Ross and Weddell seas, with smaller losses (LE) or small gains (LE-fixO3) in the Amundsen–Bellingshausen sector (Figures 1d and 1f). This pattern is apparent in the LE simulations with all forcings and can largely be attributed to the role of ozone as diagnosed from the LE-fixO3 simulations. The observed sea ice changes (red dots) show large gains in the western Ross and Weddell seas countered by losses in the Amundsen–Bellingshausen sector. This dramatic discrepancy between the modeled and the observed SIC change patterns suggests that either the model does not adequately capture the relationships between sea ice, the ASL, and ozone loss or ozone depletion is not responsible for the observed trends. We address these questions in the next section.

#### 3.2. Observed and Simulated ASL and ASL-SIC Relationships

Given that ozone loss influences the depth of the ASL (England et al., 2016) in DJF and that the ASL significantly impacts regional winds, surface temperatures, and sea ice variations (e.g., Coggins & McDonald, 2015; Hosking et al., 2013; Raphael & Hobbs, 2014; Raphael et al., 2016; Turner et al., 2009), the ASL seems an obvious candidate for mediating how ozone loss influences regional sea ice. In DJF, the ASL central pressure on average lies in the region of the Amundsen–Bellingshausen seas, and there is general agreement in magnitude and shape between observed and modeled DJF-ASL (Figures 2a and 2b; pattern correlation of 0.91). The ASL in the model is somewhat broader and shallower than in the ERA-I. This difference may be due to the large difference in the number of years used for the analysis (1,800 for the model and 26 for the observations) and the possibility of undersampling longer-term variability in the observational record. We stress that we here only consider the ASL in DJF since this is the season for which ozone depletion would impact the ASL.

The regression of SLP and winds on the ASL in DJF, shown in Figures 2c and 2d, shows good agreement between the model and the observations. Additional analysis (not shown) indicates that although the regression of SLP and winds obtained from the long PI control runs has a center of variability eastward of that seen

MAM

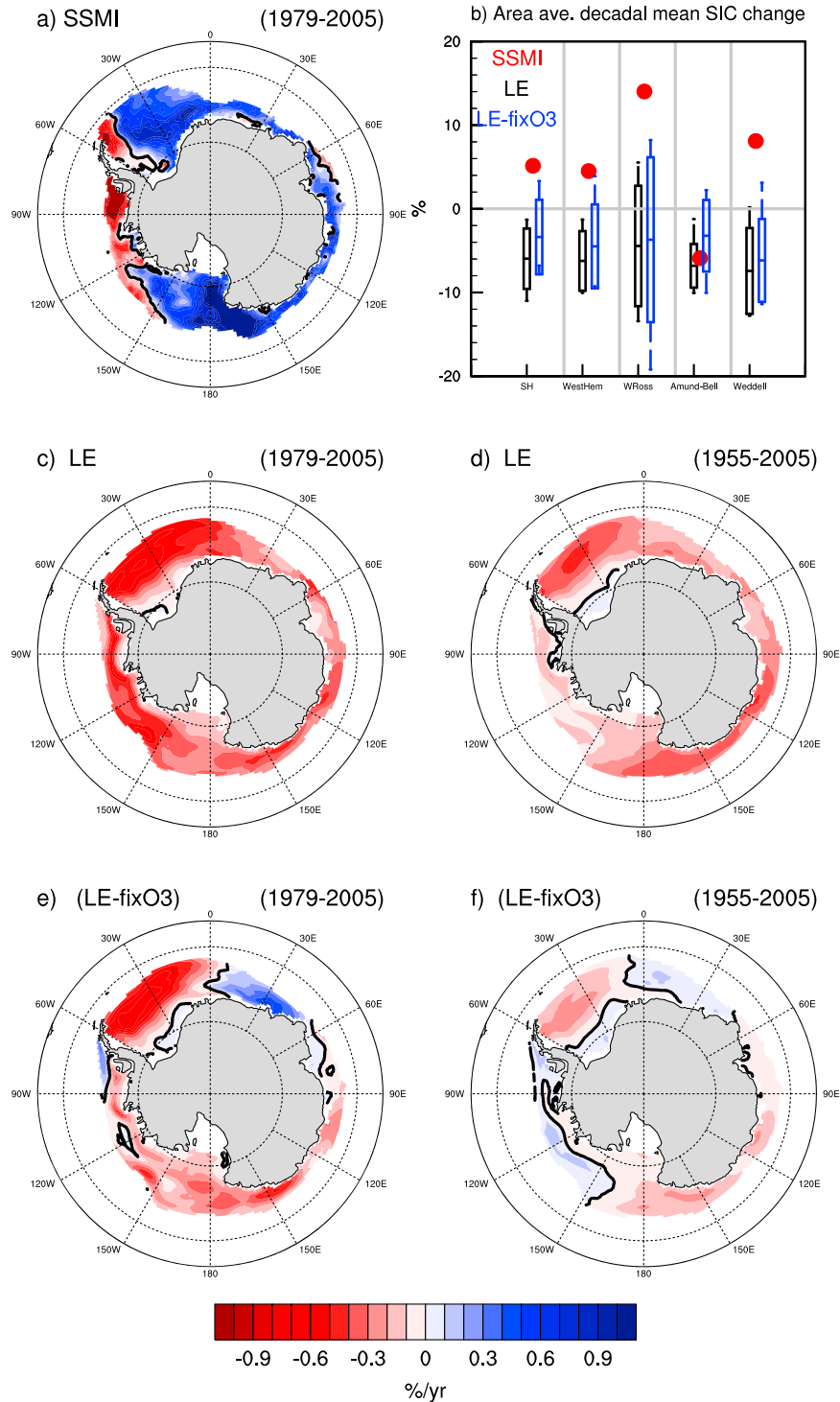


**Figure 1.** Late twentieth century sea ice concentration trends: (a) 1979–2005 SSMI observations; (c) CESM-LE ensemble mean, 1979–2005; (d) CESM-LE ensemble mean, 1955–2005; (e) ozone-attributed (LE-fixO3), 1979–2005; (f) ozone-attributed (LE-fixO3), 1955–2005; and (b) regional area-averaged late twentieth century decadal ((1996–2005)–(1979–1988)) ice concentration changes for the CESM-LE (black) and CESM ozone-attributed (blue). Boxed areas show ensemble mean and  $\pm 1$  standard deviation; dashed lines indicate the minimum and maximum individual simulations. Regions are the entire Southern Hemisphere (SH), the Western Hemisphere (149°E–360°E, “WestHem”), western Ross Sea (149°–197°E, “WRoss”), Amundsen–Bellingshausen seas (210–291°E, “Amund-Bell”), and the Weddell Sea (310–360°E, “Weddell”). Changes in the SSMI Bootstrap observations for (1996–2005)–(1979–1988) are shown by red dots for comparison. Grid cells with less than 10% ice concentration have been masked out in maps and for calculating area averages.

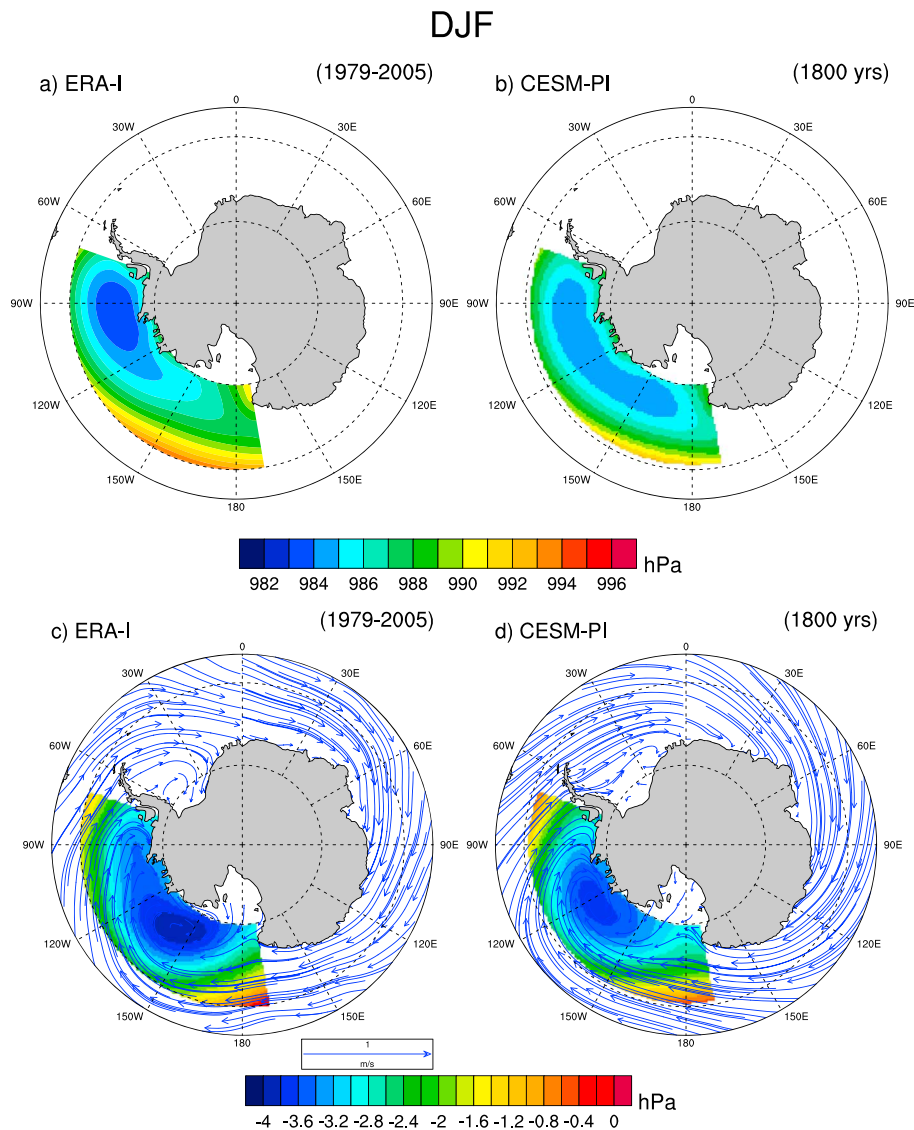


**Figure 2.** Austral summer (DJF) mean sea level pressure (SLP) in the region of the Amundsen Sea Low (ASL), 170–290°E and 60–75°S for (a) 1979–2005 ERA-I reanalysis, (b) CESM PI; regression of SLP (contours) and DJF winds (blue arrows) on the  $-1 \times \text{ASL-ACP}$  (absolute central pressure at lowest pressure in the region) for (c) ERA-I and (d) CESM PI. SLP and winds shown are those DJF associated with an anomalously low ASL (1 std decrease in absolute central pressure).

in the ERA-I reanalysis, one can find 26 year periods in the PI when the center is closer to that in the observations. This suggests that some discrepancies between the model and the observations may be due to the relatively short sampling period of the satellite era.

As shown in England et al. (2016), the only significant ozone-induced ASL changes occur in DJF in our model, whereas the largest observed SIC trends are found in MAM. We now investigate relationships between the ASL in DJF and the SIC in MAM, in both the model and the observations. Interannual correlations between the ASL in DJF and SIC in the following austral fall (MAM) are shown in Figures 3a and 3b. The regional correlation patterns in the observations and in the model are broadly similar (the pattern correlation is 0.54), except in the eastern Antarctic region (~90–160°E). These correlations indicate that with a deeper DJF-ASL, less sea ice is found in the following MAM in the Weddell Sea/Antarctic Peninsula and inner (poleward) Ross Sea, but considerably more sea ice is found in the outer (equatorward) Ross Sea and in the Amundsen Sea.

To assess if these interannual correlations between the DJF-ASL and MAM-SIC also hold for longer timescale and trends, we calculate correlations using decadal means and 40 year trends (Figures 3c and 3d). These

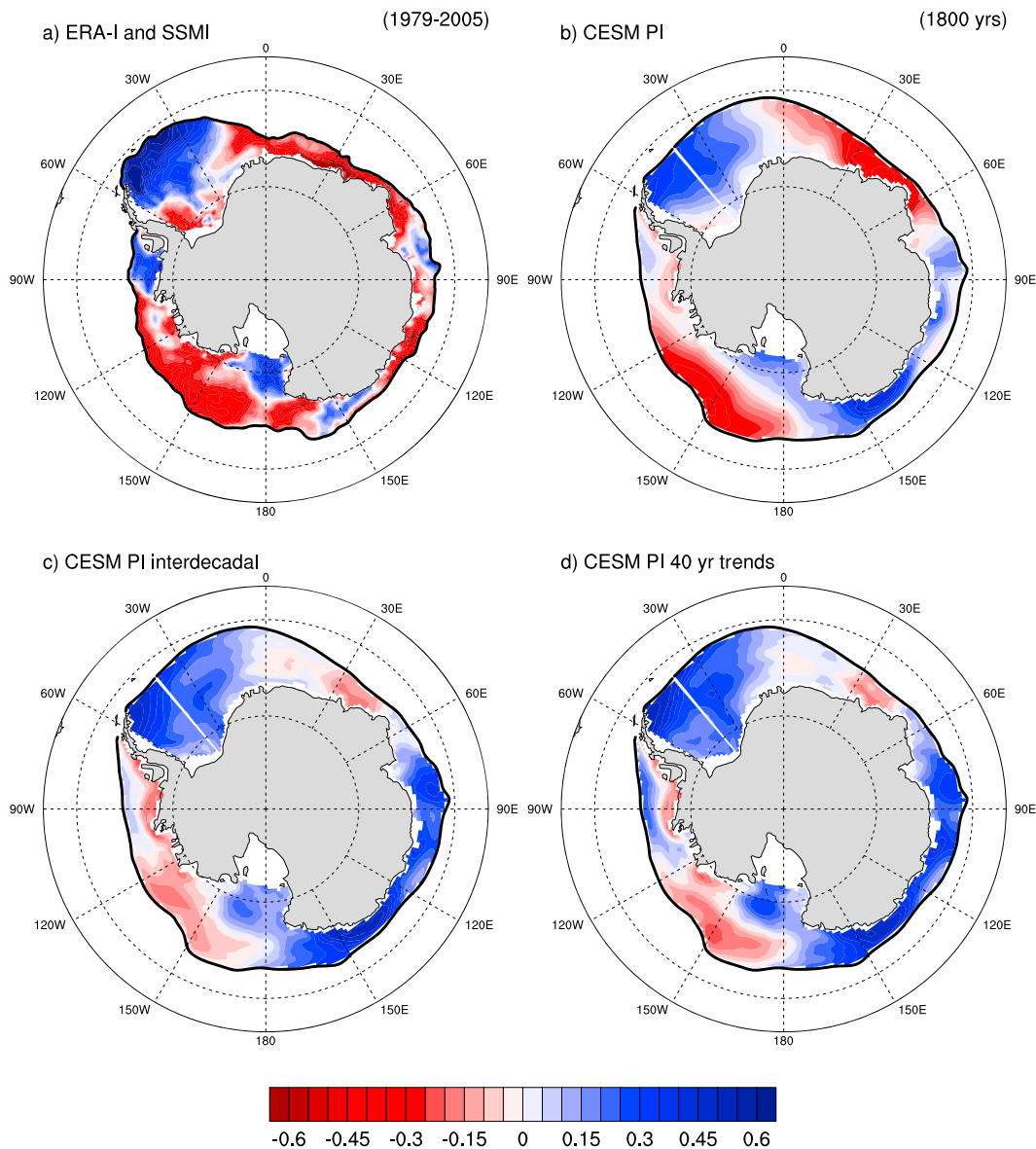


**Figure 3.** DJF ASL central pressure and fall (MAM) SIC correlations for (a) SSMI Bootstrap observations, 1979–2005, and CESM-PI (b) interannual, (c) interdecadal, and (d) 40 year trends. Negative correlations indicate regions of anomalously high sea ice concentration associated with deepening ASL. The black contour in each correlation map indicates the mean MAM 15% SIC.

correlations bear strong resemblance to the interannual correlations, suggesting consistency between interannual, interdecadal, and 40 year trend relationships in the model (the satellite observational period is insufficiently long to calculate interdecadal or trend correlations). Correlation maps using the LE and fixO3 simulations indicate that the interannual DJF-ASL:MAM-SIC relationships are very similar in the twentieth century (see supporting information Figure S1). Figure 3 provides strong evidence that the relationship between the DJF-ASL and the MAM-SIC is very robust in our model, across a wide range of timescales, and is in reasonable agreement with the observed relationship.

We now quantify the regional impacts of a deepening DJF-ASL on MAM-SIC. Modeled changes in MAM-SIC between the decades 1966–2005 and 1955–1964 are shown with the SH mean removed to highlight the regional patterns (Figure 4a). The corresponding figure for the difference between the two model ensembles (Figure 4b) shows the component of the regional MAM-SIC changes that can be attributed to ozone depletion in our model. Notice the strong resemblance between Figures 4a and 4b, indicating that a large fraction of the regional MAM-SIC changes in our model is indeed due to ozone depletion.

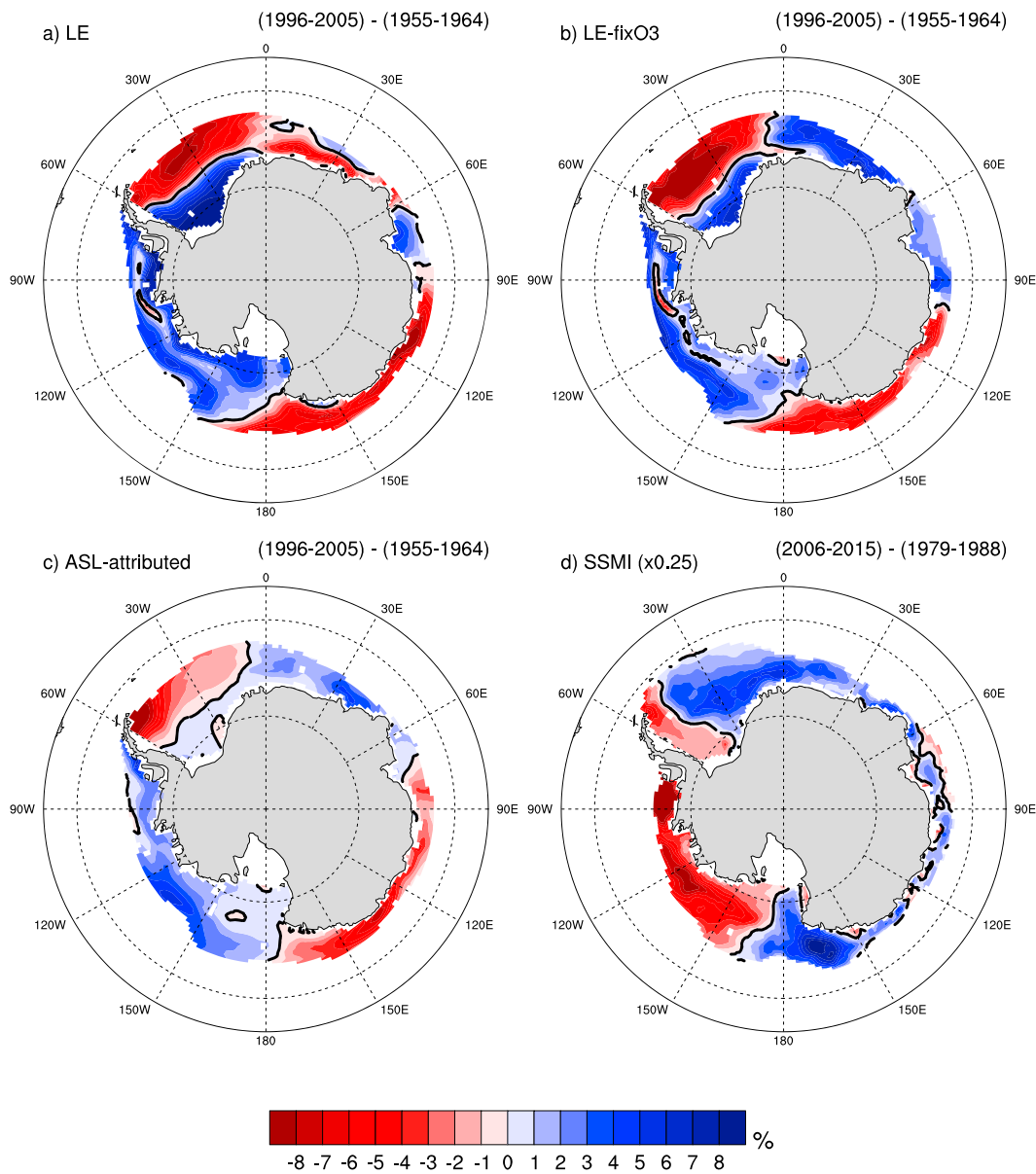


**Figure 4.** Decadal mean changes in sea ice concentration after removing hemispheric mean for (a) CESM-LE, (b) ozone-attributed (LE-fixO3), (c) ASL-attributed, and (d) SSMI bootstrap observations. CESM mean ice changes are for (1996–2005)–(1955–1964), and SSMI changes are for (2006–2015)–(1979–1988). SSMI changes have been scaled by a factor of 0.25.

Using the regression coefficients calculated from the CESM-PI interdecadal analysis, we compute the MAM-SIC changes that are associated with changes in the DJF-ASL between the early and late decades in the LE integrations. These are shown in Figure 4c and are labeled “ASL attributed.” Notice the similarity of pattern and sign between Figures 4c and 4b, from which we deduce that much of the ozone-attributed changes in our model are indeed mediated by the ASL, as one might expect from the results of Figure 3.

The surprising result comes from Figure 4d, which shows the observed regional changes: these are almost completely opposite in sign to those shown in Figures 4a, 4b, and 4c. Since the model is able to capture the ASL/SIC correlation patterns on interannual and longer timescales and since the simulated ASL responds as expected to stratospheric ozone loss, that is, it deepens (England et al., 2016), we are led to conclude that it is unlikely that the observed regional changes in SIC during MAM are caused by ozone depletion via changes in the ASL in DJF.

#### 4. Discussion and Summary

Using two ensembles and one long PI control run from a state-of-the-art fully coupled climate model, we demonstrate that the ozone loss over the last half of the twentieth century leads to regional changes in austral fall sea ice. Comparison with observations indicates that our model captures characteristics of both the climatological ASL and the interannual relationships between summer ASL and the following MAM sea ice. The model also simulates robust trends in summer ASL due to stratospheric ozone loss, and these ASL trends drive regional sea ice trends. However, the simulated regional sea ice trends are found to be largely opposite to the observed trends, suggesting that stratospheric ozone loss is an unlikely driver for observed trends.

Like most CMIP5 models, the CESM-LE simulates overall ice loss throughout the Southern Hemisphere in recent decades, in contrast to the observations. This is true for the ensemble mean and all individual members, suggesting that the discrepancy cannot be clearly attributed to internal variability. Instead, we speculate that the Southern Ocean may respond too strongly to radiative forcing from rising greenhouse gas concentrations. This is consistent with previous results that indicate that the CESM-CAM5 exhibits a relatively strong climate sensitivity (within the upper bounds of the range of CMIP5 models) and relatively slow oceanic heat uptake (Kay et al., 2015; Meehl et al., 2013). Ocean circulation and/or the direct influence of greenhouse gases may be problematic in other climate models as well (e.g., Ferreira et al., 2015; Holland et al., 2016; Sallée et al., 2013). We expect that these factors affect the hemispheric mean ice response in the twentieth century but have limited influence on the regionality of sea ice changes associated with ozone loss that is the subject of this current study.

While our work suggests that stratospheric ozone loss is an unlikely driver of regional MAM sea ice trends, the actual cause of the regionality in the observed trends remains largely unknown. A recent observational analysis indicates that autumn sea ice is more strongly related to zonal winds in the preceding October (Holland et al., 2017) than with the DJF-ASL described here. The relationship of sea ice with October winds tends to be weaker in climate models—including the CESM—than in the observations (Holland et al., 2017) and may help explain some of the regional discrepancies between observed and simulated sea ice trends in the western Ross Sea. Or, more simply, the observed trends may be a manifestation of unforced internal variability, as suggested by recent studies (Gagne et al., 2015; Polvani & Smith, 2013). Needless to say, much work remains.

#### Acknowledgments

This work is funded by a Frontiers of Earth System Dynamics (FESD) grant from the U. S. National Science Foundation (1338814). The computations were carried out with high-performance computing support from Yellowstone (ark:/85065/d7wd3xhc) provided by the National Center for Atmospheric Research's (NCAR) Computational and Information Systems Laboratory (CISL), which is sponsored by the National Science Foundation. The data produced for and analyzed in this paper are archived on the Earth System Grid at NCAR, doi:10.5065/D6JQZQRK, and are available at [https://www.earthsystemgrid.org/dataset/ucar.cgd.cesm4.b.e11.B20LE\\_fixedO3.html](https://www.earthsystemgrid.org/dataset/ucar.cgd.cesm4.b.e11.B20LE_fixedO3.html). CESM Large Ensemble Community Project and supercomputing resources were provided by NSF/CISL/Yellowstone.

#### References

- Bitz, C. M., & Polvani, L. M. (2012). Antarctic climate response to stratospheric ozone depletion in a fine resolution ocean climate model. *Geophysical Research Letters*, *39*, L20705. <https://doi.org/10.1029/2012GL053393>
- Coggins, J. H. J., & McDonald, A. J. (2015). The influence of the Amundsen Sea Low on the winds in the Ross Sea and the surroundings: Insights from a synoptic climatology. *Journal of Geophysical Research: Atmospheres*, *120*, 2167–2189. <https://doi.org/10.1002/2014JD022830>
- Comiso, J. C. (2000). Updated 2015. Bootstrap sea ice concentrations from Nimbus-7 SMMR and DMSP SSM/I-SSMIS, version 2. [indicate subset used]. Boulder, CO: NASA National Snow and Ice Data Center Distributed Active Archive Center. <https://doi.org/10.5067/J6JQLS9EJ5HU> [date accessed].
- Dee, D., Uppala, S., Simmons, A., Berrisford, P., Poli, P., Kobayashi, S., & Vitart, F. (2011). The ERA-Interim reanalysis: Configuration and performance of the data assimilation system. *Quarterly Journal of the Royal Meteorological Society*, *137*, 553–597.
- ECMWF (European Centre for Medium-Range Weather Forecasts) (2012). updated monthly. ERA-Interim Project, single parameter 6-hourly surface analysis and surface forecast time series. Research data archive at the National Center for Atmospheric Research, Computational and Information Systems Laboratory. <https://doi.org/10.5065/D64747WN>
- England, M. R., Polvani, L. M., Smith, K. L., Landrum, L., & Holland, M. (2016). Robust response of the Amundsen Sea Low to stratospheric ozone depletion. *Geophysical Research Letters*, *43*, 8207–8213. <https://doi.org/10.1002/2016GL070055>
- Ferreira, D., Marshall, J., Bitz, C. M., Solomon, S., & Plumb, A. (2015). Antarctic Ocean and sea ice response to ozone depletion: A two-time-scale problem. *Journal of Climate*, *28*, 1206–1226. <https://doi.org/10.1175/JCLI-D-14-00313.1>
- Fogt, R. L., Perlwitz, J., Monaghan, A., Bromwich, D., Jones, J., & Marshall, G. (2009). Historical SAM variability. Part II: Twentieth-century variability and trends from reconstructions, observations, and the IPCC AR4 models. *Journal of Climate*, *22*, 5346–5365.
- Gagne, M., Gillett, N., & Fyfe, J. (2015). Observed and simulated changes in Antarctic sea ice extent over the past 50 years. *Geophysical Research Letters*, *42*, 90–95. <https://doi.org/10.1002/303%202014GL062231>
- Hobbs, W. R., Massom, R., Stammerjohn, S., Reid, P., Williams, G., & Meier, W. (2016). A review of recent changes in Southern Ocean sea ice, their drivers and forcings. *Global and Planetary Change*, *143*, 228–250. <https://doi.org/10.1016/j.gloplacha.2016.06.008>
- Holland, M. M., Landrum, L., Kostov, Y., & Marshall, J. (2016). Sensitivity of Antarctic sea ice to the Southern Annular Mode in coupled climate models. *Climate Dynamics*. <https://doi.org/10.1007/s00382-016-3424-9>
- Holland, M. M., Landrum, L., Raphael, M., & Stammerjohn, S. (2017). Springtime winds drive Ross sea ice variability and change in the following autumn. *Nature Communications*, *8*(1), 731. <https://doi.org/10.1038/s41467-017-00820-0>
- Hosking, J. S., Orr, A., Marshall, G. J., Turner, J., & Phillips, T. (2013). The influence of the Amundsen–Bellingshausen seas low on the climate of West Antarctica and its representation in coupled climate model simulations. *Journal of Climate*, *26*, 6633–6648. <https://doi.org/10.1175/JCLI-D-12-00813.1>

- Hurrell, J. W., Holland, M. M., Gent, P. R., Ghan, S., Kay, J. E., Kushner, P. J., ... Marshall, S. (2013). The Community Earth System Model. *Bulletin of the American Meteorological Society*. <https://doi.org/10.1175/BAMS-D-12-00121.1>
- Kay, J. E., Deser, C., Phillips, A., Mai, A., Hannay, C., Strand, G., ... Vertenstein, M. (2015). The Community Earth System Model (CESM) Large Ensemble project: A community resource for studying climate change in the presence of internal climate variability. *Bulletin of the American Meteorological Society*, *96*, 1333–1349. <https://doi.org/10.1175/BAMS-D-13-00255.1>
- Lefebvre, W., Goosse, H., Timmermann, R., & Fichefet, T. (2004). Influence of the Southern Annular Mode on the sea-ice system. *Journal of Geophysical Research*, *109*, C09005. <https://doi.org/10.1029/2004JC002403>
- Meehl, G. A., Washington, W. M., Arblaster, J. M., Hu, A., Teng, H., Kay, J. E., ... Strand, W. G. (2013). Climate change projections in CESM1(CAM5) compared to CCSM4. *Journal of Climate*, *26*(17), 6287–6308. <https://doi.org/10.1175/JCLI-D-12-00572.1>
- Polvani, L., & Smith, K. (2013). Can natural variability explain observed Antarctic sea ice trends? New modelling evidence from CMIP5. *Geophysical Research Letters*, *40*, 3195–3199. <https://doi.org/10.1002/grl.50578>
- Polvani, L., Waugh, D., Correa, G., & Son, S. (2011). Stratospheric ozone depletion: The main driver of twentieth-century atmospheric circulation changes in the Southern Hemisphere. *Journal of Climate*, *24*, 795–812. <https://doi.org/10.1175/2010JCLI3772.1>
- Previdi, M., & Polvani, L. M. (2014). Climate system response to stratospheric ozone depletion and recovery. *Quarterly Journal of the Royal Meteorological Society*, *140*(685), 2401–2419. <https://doi.org/10.1002/qj.2330>
- Raphael, M. N., & Hobbs, W. (2014). The influence of the large-scale atmospheric circulation on Antarctic sea ice during ice advance and retreat seasons. *Geophysical Research Letters*, *41*, 5037–5045. <https://doi.org/10.1002/2014GL060365>
- Raphael, M. N., Marshall, G. J., Turner, J., Fogt, R. L., Schneider, D., Dixon, D. A., ... Hobbs, W. R. (2016). The Amundsen Sea Low variability, change, and impact on Antarctic climate. *Bulletin of the American Meteorological Society*, *97*, 111–121. <https://doi.org/10.1175/BAMS-D-14-00018.1>
- Sallée, J. B., Shuckburgh, E., Bruneau, N., Meijers, A. J. S., Bracegirdle, T. J., Wang, Z., & Roy, T. (2013). Assessment of Southern Ocean water mass circulation and characteristics in CMIP5 models: Historical bias and forcing response. *Journal of Geophysical Research: Oceans*, *118*, 1830–1844. <https://doi.org/10.1002/jgrc.20135>
- Sigmond, M., & Fyfe, J. C. (2010). Has the ozone hole contributed to increased Antarctic sea ice? *Geophysical Research Letters*, *37*, L18502. <https://doi.org/10.1029/2010GL044301>
- Sigmond, M., & Fyfe, J. C. (2014). The Antarctic sea ice response to the ozone hole in climate models. *Journal of Climate*, *27*, 1336–1342. <https://doi.org/10.1175/JCLI-D-13-00590.1>
- Smith, K. L., Polvani, L. M., & Marsh, D. R. (2012). Mitigation of 21st century Antarctic sea ice loss by stratospheric ozone recovery. *Geophysical Research Letters*, *39*, L20701. <https://doi.org/10.1029/2012GL053325>
- Thompson, D., Solomon, S., Kushner, P., England, M., Grise, K., & Karoly, D. (2011). Signatures of the Antarctic ozone hole in Southern Hemisphere surface climate change. *Nature Geoscience*, *4*, 741–749.
- Turner, J., Comiso, J. C., Marshall, G. J., Lachlan-Cope, T. A., Bracegirdle, T., Maksym, T., ... Orr, A. (2009). Non-annular atmospheric circulation change induced by stratospheric ozone depletion and its role in the recent increase of Antarctic sea ice extent. *Geophysical Research Letters*, *36*, L08502. <https://doi.org/10.1029/2009GL037524>
- Turner, J., Hosking, J. S., Bracegirdle, T. J., Marshall, G. J., & Phillips, T. (2015). Recent changes in Antarctic sea ice. *Philosophical Transactions of the Royal Society A*, *373*, 20140163. <https://doi.org/10.1098/rsta.2014.0163>
- Turner, J., Phillips, T., Hosking, J., Marshall, G., & Orr, A. (2013). The Amundsen Sea low. *International Journal of Climatology*, *33*(7), 1818–1829. <https://doi.org/10.1002/joc.3558>